

1 **Expression of extracellular multiheme cytochromes discovered in a**
2 **betaproteobacterium during Mn(III) reduction**

3 Nadia Szeinbaum^{1,2,5*}, Brook L. Nunn³, Amanda R. Cavazos², Sean A. Crowe³, Frank J.
4 Stewart¹, Thomas J. DiChristina¹, Christopher T. Reinhard^{2,5}, and Jennifer B. Glass^{2,5*}

5
6 ¹School of Biological Sciences, Georgia Institute of Technology, Atlanta, GA, USA

7 ²School of Earth and Atmospheric Sciences, Georgia Institute of Technology, Atlanta, GA, USA

8 ³Department of Genome Sciences, University of Washington, Seattle, WA, USA

9 ⁴Department of Microbiology & Immunology and Department of Earth, Ocean, & Atmospheric
10 Sciences, University of British Columbia, Vancouver, Canada

11 ⁵NASA Astrobiology Institute, Alternative Earths Team, Mountain View, CA

12

13 *Corresponding author: jennifer.glass@eas.gatech.edu

14 **Running title:** Novel undecaheme in Betaproteobacteria

15

16 **Abstract:** Soluble ligand-bound Mn(III) can support anaerobic microbial respiration in diverse
17 aquatic environments. Thus far, Mn(III) reduction has only been associated with certain
18 *Gammaproteobacteria*. Here, we characterized microbial communities enriched from Mn-replete
19 sediments of Lake Matano, Indonesia. Our results provide the first evidence for biological
20 reduction of soluble Mn(III) outside of the *Gammaproteobacteria*. Metagenome assembly and
21 binning revealed a novel betaproteobacterium, which we designate “*Candidatus* Dechloromonas
22 occultata.” This organism dominated the enrichment and expressed a novel cytochrome c-rich
23 protein cluster (Occ), including an undecaheme putatively involved in extracellular electron
24 transfer during Mn(III) reduction. The *occ* gene cluster was detected in diverse aquatic bacteria,
25 including uncultivated *Betaproteobacteria* from the deep subsurface. These observations provide
26 new insight into the taxonomic and functional diversity of microbially-driven Mn(III) reduction
27 in natural environments.

28
29 **Main text:** Manganese(III) is the most recently discovered player in the manganese cycle (10).
30 Ligand-bound Mn(III) is often the most abundant Mn species in aquatic ecosystems (18), yet
31 knowledge about microbes cycling Mn(III) remains fragmentary. To date, only *Shewanella* spp.
32 (*Gammaproteobacteria*) are known to respire soluble Mn(III) using the Mtr pathway (17, 22,
33 23). The Mtr pathway forms a porin-cytochrome (PCC) conduit that transports electrons across
34 the periplasm (11) for extracellular respiration of Mn(III/IV), Fe(III), and other metals (20, 23).
35 Another PCC is Mto used by freshwater *Betaproteobacteria* for extracellular Fe(II) oxidation (7,
36 12, 16). Environmental omics suggests that metal reduction by *Betaproteobacteria* may be
37 widespread in the deep subsurface (1, 13). However, only a few Fe(III)-reducing
38 *Betaproteobacteria* isolates have been characterized (5, 8). This study presents the first evidence

39 for biological reduction of soluble Mn(III) by a bacterium outside of the *Gammaproteobacteria*
40 class.

41 We explored microbial Mn(III) reduction in enrichments inoculated with sediment from
42 Lake Matano, Indonesia, which has active microbial Mn and methane (CH₄) cycles (15).
43 Manganese reduction coupled to CH₄ oxidation is a thermodynamically favorable metabolism,
44 and its natural occurrence is supported by biological evidence (2) and geochemical evidence (4,
45 19). We designed an enrichment strategy to select for microbes capable of anaerobic CH₄
46 oxidation coupled to soluble Mn(III) reduction incubating anoxic Lake Matano with soluble
47 Mn(III)-pyrophosphate as the electron acceptor (with 2% O₂ in a subset of bottles), and CH₄ as
48 the sole electron donor and carbon source (see **Supplemental Material** for enrichment details).
49 Cultures were transferred into fresh media after Mn(III) was completely reduced to Mn(II) for a
50 total of five transfers over 395 days. By the fourth transfer, cultures with CH₄ headspace (with or
51 without 2% O₂) reduced ~80% of soluble Mn(III) compared to ~30% with N₂ headspace (**Fig. 1**).
52 16S rRNA gene sequences were dominated by *Betaproteobacteria* (*Rhodocyclales*) and
53 *Deltaproteobacteria* (*Desulfuromonadales*), and ¹³CH₄ oxidation to ¹³CO₂ was undetectable
54 (**Figs. S1, S2**).

55 Samples for metagenomic and metaproteomic analysis were harvested from the fifth
56 transfer (**Fig. 1; Fig. S1**). Out of 2,952 proteins identified in the proteome, 90% were assigned to
57 *Betaproteobacteria*; of those, 72% mapped to a 99.53% metagenome-assembled genome (MAG;
58 *Rhodocyclales* bacterium GT-UBC; NCBI accession QXPY01000000) with 81-82% average
59 nucleotide identity (ANI) and phylogenetic affiliation to *Dechloromonas* spp. (**Table S1; Fig.**
60 **S3**). This MAG is named here “*Candidatus Dechloromonas occultata*” sp. nov.; etymology:
61 *occultata*; (L. fem. adj. ‘hidden’). The remaining 10% of proteins mapped to

62 *Deltaproteobacteria*; of those, 70% mapped to a nearly complete MAG (*Desulfuromonadales*
63 bacterium GT-UBC; NCBI accession RHLS01000000) with 80% ANI to *Geobacter*
64 *sulfurreducens*. This MAG is named here “*Candidatus Geobacter occultata*”.

65 Cytochromes containing multiple *c*-type hemes are key for electron transport during
66 microbial metal transformations, and therefore might also be expected to play a role in Mn(III)
67 reduction. Numerous mono-, di-, and multi (>3)-heme cytochromes (MHCs) were expressed by
68 “*Ca. D. occultata*” in Mn(III)-reducing cultures. Nine out of 15 MHCs encoded by the “*Ca. D.*
69 *occultata*” MAG were expressed, including two decahemes similar to MtoA in Fe(II)-oxidizing
70 *Betaproteobacteria* (**Tables 1, S2, S3; Figs. 2A, S4**). Several highly expressed MHCs were
71 encoded on a previously unreported 19-gene cluster with 10 cytochrome-*c* proteins, hereafter
72 *occA-S* (**Table 1; Figs. 2B, S5, S6**). OccP was an undecaheme, which are known to be involved
73 in metal reduction (6, 21). “*Ca. Dechloromonas occultata*” may reduce Mn(III) using the novel
74 extracellular undecaheme OccP as the terminal Mn(III) reductase, although the function of the
75 putative Occ complex has yet to be experimentally verified.

76 We investigated the taxonomic distribution of genes encoding *occP*, *mtoA*, and key
77 denitrification complexes expressed by “*Ca. D. occultata*”. We discovered *occP* homologs (40-
78 60% identity) in diverse *Betaproteobacteria* from diverse freshwaters and deep subsurface
79 groundwaters, as well as several *Gammaproteobacteria* and one alphaproteobacterium (**Fig. 2D;**
80 **Table S3**). Most *occP*-containing bacteria also possessed *mtoA* and denitrification (**Fig. 2D**)
81 genes. For more discussion of denitrification, see **Supplemental Text** and **Figs. S7** and **S8**.

82 While the specific role of CH₄ in Mn(III) reduction remains unknown (see **Supplemental**
83 **Text**), CH₄ significantly stimulated expression of many cytochrome *c* proteins, including
84 OccABGJK, MtoD-2, and cytochrome-*c*4 and -*c*5 proteins associated with anaerobic respiration

85 (p < 0.05; **Table 1; Fig. 2C**). Methane also led to increased expression of several “*Ca. D.*
86 *occultata*” proteins involved in outer membrane structure and composition, including an
87 extracellular DUF4214 protein located next to an S-layer protein similar to those involved in
88 manganese binding and deposition (24), a serine protease possibly involved in Fe(III) particle
89 attachment (3), an extracellular PEP-CTERM sorting protein for protein export (9), and a Tol-Pal
90 system for outer membrane integrity (**Table 1**). A type IV pilin protein (87% identity to
91 *Geobacter pickeringii* (14)) was significantly more highly expressed with CH₄ vs. N₂ in the “*Ca.*
92 *G. occultata*” proteome (p=0.02; **Table 1**). The possible involvement of *Geobacter* e-pilins in
93 Mn(III) reduction remains an open question. For additional discussion of other features of “*Ca.*
94 *D. occultata*” and “*Ca. G. occultata*” genomes and proteomes, see **Supplemental Text, Table**
95 **S4**, Figs. **S9**, **S10**, and **S11**.

96
97 **Acknowledgements.** This research was funded by NASA Exobiology grant NNX14AJ87G.
98 Support was also provided by a Center for Dark Energy Biosphere Investigations (NSF-CDEBI
99 OCE-0939564) small research grant and supported by the NASA Astrobiology Institute
100 (NNA15BB03A) and a NASA Astrobiology Postdoctoral Fellowship to NS. SAC was supported
101 through NSERC CRC, CFI, and Discovery grants. We thank Marcus Bray, Andrew Burns, Caleb
102 Easterly, Pratik Jagtap, Cory Padilla, Angela Peña, Johnny Striepen, and Rowan Wolschleger for
103 technical assistance. We thank Emily Weinert for helpful discussions.

104

105 **Competing Interests:** The authors declare no competing interests.

106

107 **References**

- 108 1 Anantharaman K, Brown CT, Hug LA, Sharon I, Castelle CJ, Probst AJ *et al* (2016). Thousands
109 of microbial genomes shed light on interconnected biogeochemical processes in an aquifer system. *Nat*
110 *Commun* **7**: 13219.
- 111 2 Beal EJ, House CH, Orphan VJ (2009). Manganese- and iron-dependent marine methane
112 oxidation. *Science* **325**: 184-187.
- 113 3 Burns JL, Ginn BR, Bates DJ, Dublin SN, Taylor JV, Apkarian RP *et al* (2009). Outer
114 membrane-associated serine protease involved in adhesion of *Shewanella oneidensis* to Fe (III) oxides.
115 *Environmental science & technology* **44**: 68-73.
- 116 4 Crowe SA, Katsev S, Leslie K, Sturm A, Magen C, Nomosatryo S *et al* (2011). The methane
117 cycle in ferruginous Lake Matano. *Geobiology* **9**: 61-78.
- 118 5 Cummings DE, Caccavo F, Spring S, Rosenzweig RF (1999). *Ferribacterium limneticum*, gen.
119 nov., sp. nov., an Fe(III)-reducing microorganism isolated from mining-impacted freshwater lake
120 sediments. *Archives of Microbiology* **171**: 183-188.
- 121 6 Edwards MJ, Hall A, Shi L, Fredrickson JK, Zachara JM, Butt JN *et al* (2012). The crystal
122 structure of the extracellular 11-heme cytochrome UndA reveals a conserved 10-heme motif and defined
123 binding site for soluble iron chelates. *Structure* **20**: 1275-1284.
- 124 7 Emerson D, Field EK, Chertkov O, Davenport KW, Goodwin L, Munk C *et al* (2013).
125 Comparative genomics of freshwater Fe-oxidizing bacteria: implications for physiology, ecology, and
126 systematics. *Front Microbiol* **4**: 254.
- 127 8 Finneran KT, Johnsen CV, Lovley DR (2003). *Rhodoferrax ferrireducens* sp. nov., a
128 psychrotolerant, facultatively anaerobic bacterium that oxidizes acetate with the reduction of Fe(III).
129 *International Journal of Systematic and Evolutionary Microbiology* **53**: 669-673.
- 130 9 Haft DH, Paulsen IT, Ward N, Selengut JD (2006). Exopolysaccharide-associated protein sorting
131 in environmental organisms: the PEP-CTERM/EpsH system. Application of a novel phylogenetic
132 profiling heuristic. *BMC Biol* **4**: 29.
- 133 10 Hansel C (2017). Small but mighty: how minor components drive major biogeochemical cycles.
134 *Environmental microbiology reports* **9**: 8-10.
- 135 11 Hartshorne RS, Reardon CL, Ross D, Nuester J, Clarke TA, Gates AJ *et al* (2009).
136 Characterization of an electron conduit between bacteria and the extracellular environment. *Proc Natl*
137 *Acad Sci U S A* **106**: 22169-22174.
- 138 12 He S, Barco RA, Emerson D, Roden EE (2017). Comparative Genomic Analysis of Neutrophilic
139 Iron (II) Oxidizer Genomes for Candidate Genes in Extracellular Electron Transfer. *Frontiers in*
140 *Microbiology* **8**: 1584.
- 141 13 Hermsdorf AW, Amano Y, Miyakawa K, Ise K, Suzuki Y, Anantharaman K *et al* (2017).
142 Potential for microbial H₂ and metal transformations associated with novel bacteria and archaea in deep
143 terrestrial subsurface sediments. *The ISME Journal* **11**: 1915.
- 144 14 Holmes DE, Dang Y, Walker DJ, Lovley DR (2016). The electrically conductive pili of
145 *Geobacter* species are a recently evolved feature for extracellular electron transfer. *Microbial Genomics* **2**.

- 146 15 Jones C, Crowe SA, Sturm A, Leslie KL, MacLean LCW, Katsev S *et al* (2011).
147 Biogeochemistry of manganese in ferruginous Lake Matano, Indonesia. *Biogeosciences* **8**: 2977-2991.
- 148 16 Kato S, Ohkuma M, Powell DH, Krepski ST, Oshima K, Hattori M *et al* (2015). Comparative
149 genomic insights into ecophysiology of neutrophilic, microaerophilic iron oxidizing bacteria. *Frontiers in*
150 *Microbiology* **6**: 1265.
- 151 17 Kostka JE, Luther III GW, Nealson KH (1995). Chemical and biological reduction of Mn (III)-
152 pyrophosphate complexes: potential importance of dissolved Mn (III) as an environmental oxidant.
153 *Geochimica et Cosmochimica Acta* **59**: 885-894.
- 154 18 Oldham VE, Siebecker MG, Jones MR, Mucci A, Tebo BM, Luther GW (2019). The Speciation
155 and Mobility of Mn and Fe in Estuarine Sediments. *Aquatic Geochemistry*.
- 156 19 Riedinger N, Formolo MJ, Lyons TW, Henkel S, Beck A, Kasten S (2014). An inorganic
157 geochemical argument for coupled anaerobic oxidation of methane and iron reduction in marine
158 sediments. *Geobiology* **12**: 172-181.
- 159 20 Shi L, Dong H, Reguera G, Beyenal H, Lu A, Liu J *et al* (2016). Extracellular electron transfer
160 mechanisms between microorganisms and minerals. *Nature Reviews Microbiology* **14**: 651.
- 161 21 Smith JA, Lovley DR, Tremblay PL (2013). Outer cell surface components essential for Fe(III)
162 oxide reduction by *Geobacter metallireducens*. *Appl Environ Microbiol* **79**: 901-907.
- 163 22 Szeinbaum N, Burns JL, DiChristina TJ (2014). Electron transport and protein secretion pathways
164 involved in Mn (III) reduction by *Shewanella oneidensis*. *Environmental Microbiology Reports* **6**: 490-
165 500.
- 166 23 Szeinbaum N, Lin H, Brandes JA, Taillefert M, Glass JB, DiChristina TJ (2017). Microbial
167 manganese(III) reduction fuelled by anaerobic acetate oxidation. *Environ Microbiol* **19**: 3475-3486.
- 168 24 Wang X, Schröder HC, Schloßmacher U, Müller WE (2009). Organized bacterial assemblies in
169 manganese nodules: evidence for a role of S-layers in metal deposition. *Geo-Marine Letters* **29**: 85-91.
- 170
171

172 **Table and Figure Captions**

173

174

175 **Table 1. Expression levels for “*Ca. D. occultata*” proteins in the presence of CH₄ and N₂.**

176 Peptide counts are normalized to total “*Ca. D. occultata*” proteins x 10,000. Blank cells indicate

177 proteins with <2 normalized peptide counts. Gray boxes indicate membrane proteins with that

178 may be underrepresented by mass spectrometry-based metaproteomic analyses, which inherently

179 favor soluble over insoluble membrane-bound or hydrophobic proteins. SP: signal peptide

180 (Y:present/N:absent); TMH: numbers of transmembrane helices; # CxxCH: number of heme-

181 binding motifs; P-sort: predicted cellular location. Bold proteins indicate proteins that were

182 significantly more expressed with CH₄ than N₂ (CH₄/N₂>1; p<0.05). MCP: methyl-accepting

183 chemotaxis protein; PPIase: Peptidyl-proline isomerase; P: periplasm, C: cytoplasm; OM: outer

184 membrane; IM: inner membrane, E: extracellular; U: unknown. MtoX and MtoY were predicted

185 to be an inner membrane cytochrome-b protein and a methyl-accepting chemotaxis protein,

186 respectively.

187

188 **Figure 1. Consumption of Mn(III) in Lake Matano enrichments in the presence and**

189 **absence of methane.** Sediment-free cultures (transfer 4) from 335 days after the initial

190 enrichment were incubated for 45 days with 1 mM Mn(III) pyrophosphate as the sole electron

191 acceptor. Initial bottle headspace contained 50% CH₄ + 50% N₂ (black circles), 50% CH₄+48%

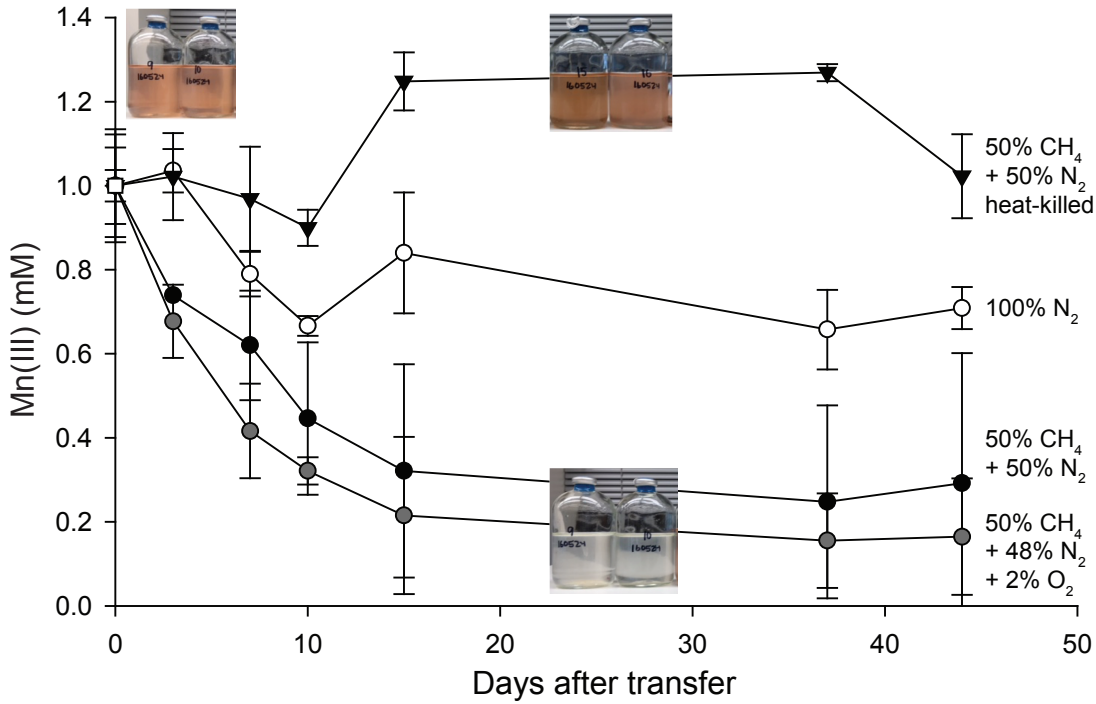
192 N₂+2% O₂ (gray circles), 100% N₂ (white circles), and 50% CH₄+50% N₂ heat killed controls

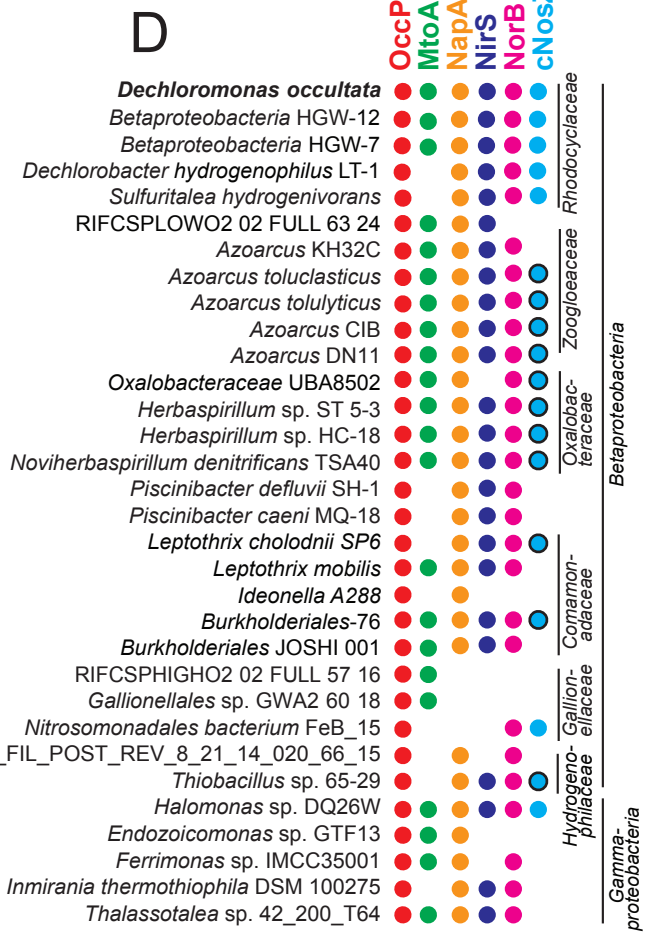
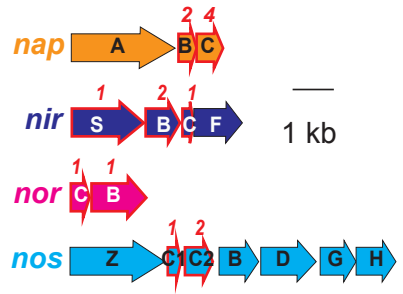
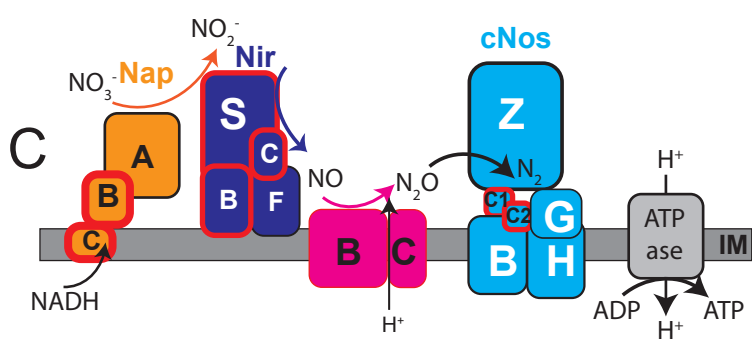
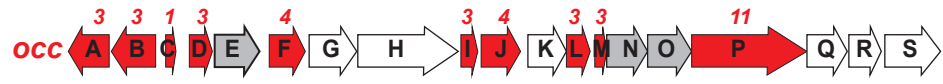
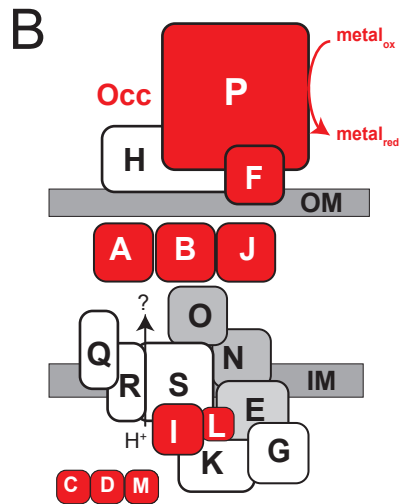
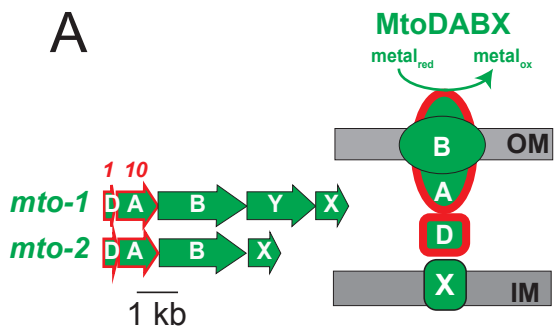
193 (black triangles). Error bars are standard deviations from duplicate experiments. Color change

194 from red to clear indicates Mn(III) reduction.

195

196 **Figure 2. Gene arrangement, predicted protein locations, and taxonomic distribution of**
197 **major expressed respiratory complexes in “*Ca. D. occultata*”.** **A:** MtoDAB(Y)X porin-
198 cytochrome c electron conduit; **B:** OccA-S; **C:** denitrification complexes (Nap, Nir, Nor and
199 cNos); **D:** Occurrence of key marker genes in *Betaproteobacteria* and *Gammaproteobacteria*
200 with >95% complete genomes that encode OccP. Red fill around genes and proteins indicate
201 cytochrome-*c* proteins. Black outlines around blue circles in D indicate type I nitrous oxide
202 reductase to distinguish from blue dots (type II/cytochrome-nitrous oxide reductase). Gray-
203 shaded genes on the *occ* gene cluster indicate 6-NHL repeat proteins. Protein locations shown
204 are based on P-sort predictions. Numbers above genes indicate number of CxxCH motifs
205 predicted to bind cytochrome *c*. IM: inner membrane; OM: outer membrane. For more details,
206 see **Table 1** and **Table S3**.





Enzyme	Function	SP	TMH	CxxCH	P-sort	NCBI ID	Normalized peptide counts				CH4/N2		P value
							CH ₄	SD	N ₂	SD	ave	SD	
<i>Ca. Dechloromonas occultata</i>													
Mto-1	MtoX-1 (cyt-b)	N	5	0	IM	RIX49676							
	MtoY-1 (MCP)	N	2	1	IM	RIX49677	2.7	0.5	3.6	0.2	0.8	0.2	0.2
	MtoB-1 (porin)	Y	0	0	OM	RIX49678	10	2	15	2	0.6	0.1	0.004
	MtoA-1	Y	1	10	P	RIX49874	5	1	2.5	0.1	1.9	0.4	0.1
	MtoD-1	N	0	1	P	RIX49875							
Mto-2	MtoX-2 (cyt-b)	N	4	0	IM	RIX48942							
	MtoB-2 (porin)	Y	0	0	OM	RIX48943	8	1	16	0.2	0.5	0.1	0.04
	MtoA-2	Y	1	10	P	RIX48944	7.3	0.8	4	2	2.1	1.3	0.2
	MtoD-2	Y	1	1	U	RIX48945	2.6	0.3	0.7	0.3	4.0	1.4	0.003
Occ	OccA	Y	1	3	P	RIX49688	4	0.5	0.7	0.6	7.8	5.7	0.01
	OccB	Y	0	3	U	RIX49689	41	4	19	2	2.2	0.0	0.03
	OccC	N	0	1	U	RIX49877							
	OccD	N	0	3	U	RIX49878							
	OccE (6-NHL)	N	1	0	U	RIX49690	22	2.1	20.5	0.2	1.1	0.1	0.2
	OccF	Y	2	4	E	RIX49691	13	0.7	10.1	0.1	1.3	0.1	0.06
	OccG (PPIase)	N	0	0	U	RIX49692	14	1	3.3	0.5	4.2	0.3	0.01
	OccH	N	0	0	OM/E	RIX49693	6.0	0.2	7.7	0.6	0.8	0.1	0.10
	OccI	N	1	3	U	RIX49694	7	2.5	2.3	0.0	2.9	1.1	0.1
	OccJ	Y	0	4	U	RIX49879	44	0.2	19	3	2.4	0.4	0.03
	OccK	N	0	0	C	RIX49880	39	6	13	1	3.0	0.2	0.04
	OccL	N	1	3	U	RIX49695							
	OccM	N	0	3	U	RIX49881							
	OccN (6 NHL)	N	2	0	U	RIX49696	5.7	0.3	6	1	0.9	0.1	0.2
	OccO (6 NHL)	N	0	0	U	RIX49882	1.2	0.8	4.2	0.4	0.3	0.2	0.03
	OccP	N	0	11	E	RIX49697	14	2	12	3	1.2	0.5	0.4
	OccQ	Y	4	0	IM	RIX49698							
OccR	N	8	0	IM	RIX49883								
OccS	N	12	0	IM	RIX49699								
Cyt c	Cyt c5	N	1	1	U	RIX47670	27	2	9	3	3.2	0.8	0.01
	Cyt c5	Y	1	2	P	RIX40984	19	2	6	1	3.3	1.0	0.06
	Cyt c'/C_2	Y	1	1	P	RIX44710	17	5	3.6	0.8	4.8	2.3	0.09
	Cyt c'/C_2	Y	1	1	P	RIX49630	7	1	1.2	0.9	8.2	6.6	0.07
	Cyt c551/c552	Y	0	1	P	RIX49087	13	3	2.8	0.0	4.8	1.1	0.06
	Cyt c4	Y	0	2	P	RIX48804	16	0.8	9.8	0.8	1.6	0.2	0.06
	Cyt c4	Y	0	2	P	RIX44782	4	2	1.7	0.7	2.6	0.1	0.08
Cyt c4	Y	0	2	P	RIX45018	7	0.6	2.2	0.2	3.0	0.0	0.02	
Nap	NapA	Y	0	0	P	RIX41011	76	2	67	3	1.1	0.1	0.1
	NapB	Y	1	2	P	RIX41010	15	1	5	2	3.2	0.9	0.02
	NapC	N	1	4	IM	RIX41009	12	3	13	1	1.0	0.2	0.1
Nir	NirS	Y	0	1	P	RIX44719	58	2	44	4	1.3	0.2	0.1
	NirB	Y	1	2	P	RIX44720	14	3	10	2	1.5	0.6	0.2
	NirC	N	0	1	P	RIX44788							
	NirF	Y	1	0	P or C	RIX44721	2	1	7	1	0.3	0.1	0.02
Nor	NorC	N	1	1	IM	RIX45182	3.5	0.7	3.2	0.7	1.1	0.0	0.1
	NorB	N	12	1	IM	RIX45183							
cNos	cNosZ	Y	0	0	P	RIX42539	77	17	66	8	1.2	0.3	0.2
	cNosC1	Y	1	1	P	RIX42538	16	2	4	2	5	3	0.08
	cNosC2	Y	1	2	P	RIX42537	10	0.1	3.9	0.3	2.6	0.1	0.02
	cNosB	N	6	0	IM	RIX42536							
	cNosD	N	0	0	P	RIX42535							
	cNosG	N	1	0	C	RIX42534							
Qcr	cNosH	N	4	0	IM	RIX42533							
	QcrA	N	9	0	CM	RIX41976							
	QcrB	N	9	0	CM	RIX41977							
	QcrC	N	1	0	CM	RIX41978							
Proteases	Serine protease	N	0	0	P	RIX49468	27	2	1.0	0.3	29	10	0.02
	Carboxyl-terminal protease (S41)	N	1	0	CM	RIX48818	18.5	0.8	8.0	0.9	2.3	0.1	0.0002
Membrane/Extracellular	DUF4214 protein	N	0	0	OM/E	RIX44180	146	25	43	0.6	3.4	0.5	0.05
	S-layer protein	N	0	0	U	RIX44181	8	0.5	10	0.6	0.8	0.1	0.14
	PEP-CTERM sorting	Y	1	0	E	RIX45463	68	6	33	10	2.1	0.5	0.03
	Tol-Pal system protein TolB	Y	0	0	P	RIX44015	20	2	12	1	1.67	0.05	0.03
	Peptidoglycan-associated lipoprotein (Pal)	N	0	0	OM	RIX44016	27.3	0.2	10	3	3	1	0.04
	Tol-Pal system protein YbgF	Y	0	0	U	RIX44017	10.8	0.4	4	2	4	2	0.06
Other	Pilus assembly protein	N	0	0	U	RIX46961	54	5	30	5	1.8	0.1	0.001
	PQQ-dependent dehydrogenase	Y	0	0	P	RIX45050	37	4	17	1	2.2	0.1	0.03
	Phasin family granule-associated protein	N	0	0	U	RIX40682	49	2	22	1	2.2	0.2	0.03
	Phasin family granule-associated protein	Y	0	0	U	RIX40683	34	4	16	1	2.1	0.0	0.03
	High potential iron-sulfur protein	Y	0	0	U	RIX49681	10.79	0.01	6.5	0.4	1.7	0.1	0.02
Electron transfer flavoprotein (FixA)	N	0	0	C	RIX43544	16	3	10	2	1.7	0.0	0.04	
<i>Ca. Geobacter occultata</i>													
E-pilus	Type IV pilin PilA	N	1	0	E	RNC67631	93	3	18	3	5	1	0.02